Applying the Phase Congruency Algorithm to Seismic Data Slices – A Carbonate Case Study

Brian Russell[1], Dan Hampson[1], and John Logel[2]

[1] Hampson-Russell, A CGGVeritas Company, Calgary, Alberta, brian.russell@cggveritas.com
dan.hampson@cggveritas.com [2] Talisman Energy Inc, Calgary, Alberta, jlogel@talisman-energy.com

Introduction

Traditionally, the analysis of seismic data involved looking for continuous events on seismic data, from which structural and stratigraphic features could be mapped. However, we are also interested in mapping discontinuous features such as faults and fractures. A method for identifying these discontinuities was first introduced by Bahorich and Farmer (1995) and called the coherency algorithm (although it is important to note that the algorithm looks for lack of coherency in the seismic data). This method, based on cross-correlation between adjacent traces, has remained the industry standard since its introduction and has undergone several major enhancements.

However, researchers in other areas of image analysis, such as robot vision and feature identification, have also been looking at ways to identify discontinuities on their images. One such development is the phase congruency algorithm (Kovesi, 1996), which is able to identify corners and edges on images of shapes and possible obstacles to enhance robot vision. In this paper, we have implemented the phase congruency algorithm in a seismic analysis toolbox and apply it to seismic data slices to look for discontinuities on these slices.

Theory of Phase Congruency

The phase congruency (PC) algorithm was developed to detect corners and edges on 2D digital images (Kovesi, 1996). To understand the concept behind phase congruency in 2D space, with x and y coordinates, it is instructive to first understand the algorithm in 1D, as illustrated in Figure 1.
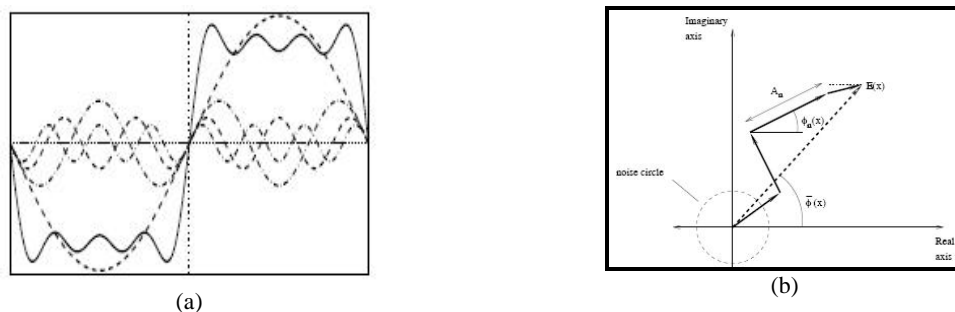

(a)   (b)

Figure 1. The concept of phase congruency in 1D, where (a) shows that the individual terms in a Fourier series will be in-phase at a step, and (b) shows a polar plot of the real and imaginary Fourier used to compute phase congruency (from Kovesi, 2003).

Figure 1(a), from Kovesi (2003), shows n individual Fourier series terms over a simple step function, where the horizontal axis is the x axis and the vertical axis is the amplitude of the Fourier terms. Note that these terms are

all in-phase at the step. To quantify this concept, we plot the real and imaginary values for all n terms and plot them in the polar plot shown in Figure 1(b). We can then draw the vectors as shown, with their related amplitude and phase values for all n terms. Kovesi (2003) shows that a simple measure of phase congruency is

$$PC(x) = \frac{|E(x)|}{\sum_n A_n(x)} = \frac{\sum_n A_n(x)\cos(\phi_n(x) - \bar{\phi}(x))}{\sum_n A_n(x)}, \tag{1}$$

where $A_n(x)$ and $\phi_n(x)$ are the length and phase angle of each of the individual n amplitude vectors, and $E(x)$ and $\bar{\phi}(x)$ are the length and phase angle of the summed vectors.

Kovesi (2003) then gives a more advanced formula that builds in a weight factor for frequency spread and a noise threshold. However, equation (1) is sufficient for an understanding of the basic algorithm. More importantly, Kovesi (2003) shows how to extend equation (1) to the two-dimensional image domain. This is done using oriented 2D Gabor wavelets in the 2D Fourier domain. In the initial implementation, Kovesi used 2D Gaussian wavelets, but in a later implementation he used log Gabor wavelets. The advantage of the log Gabor transform when used for the radial filtering is that it is Gaussian on a logarithmic scale and thus has better high frequency characteristics than the traditional Gabor transform. The first steps in the 2D phase congruency algorithm are to transform the data to the 2D Fourier domain, then apply $N*M$ filters (N radial log Gabor filters multiplied by M angular filters). The log Gabor filters are computed over N "scales" S, where $S = 0, \ldots, N\text{-}1$. Typically, the value of N is between 4 and 8. Each log Gabor filter is computed by the formula

$$\log Gabor_S = \exp\left[\frac{-\ln(r \cdot \lambda_S)^2}{\sigma}\right] \cdot lp, \tag{2}$$

where r = the radius value from the zero frequency value, λ_S is the scale value, where $\lambda_S = 3m^S$, with a default value of $m = 2.1$, $\sigma = 2\ln(0.55)^2$ and lp is a low pass 2D Butterworth filter. The angular filters are created over M orientations or angles θ, where $\theta = 0, \pi/M, \ldots, (M\text{-}1)\pi/M$. The default value of M is 6, in which case the angles will go from 0° to 150° in increments of 30°. After the $N*M$ filters are applied, each filtered image is transformed back to the spatial domain and, after appropriate weighting and noise thresholding, are summed over the scales to produce an image at each orientation. These images are then analyzed using moment analysis. The magnitude of the maximum moment indicates the significance of a feature on the image, or its "edge".

A Simple Example
Let us now look at applying phase congruency to a simple example. Since the original algorithm was developed to identify features on a 2D photographic that could be analyzed for robot vision, it was decided that a suitable example would consist of the cylinder and cube. The map view of the shapes is shown in Figure 2(a). We used 4 scales (with $m = 2.1$) and 6 orientations. The final result is shown in Figure 2(b). Notice how well that the edges of the two structures have been defined.
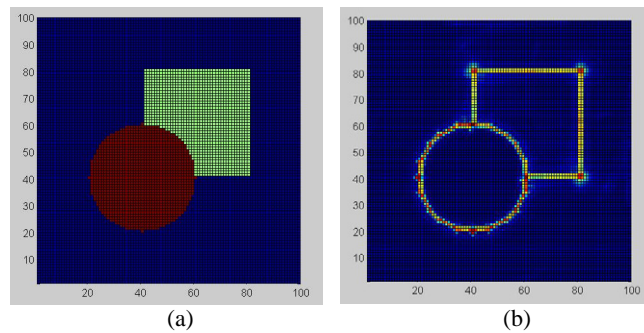

(a)   (b)

Figure 2. Map views of the (a) original image consisting of a cylinder and a cube from figure 5(b), and (b) the final analysis using phase congruency. Notice the clear definition of the edges of the two objects.

Implementation on 3D Seismic Volumes

A simple schematic diagram showing the way in which the phase congruency method was implemented on seismic data slices is shown in Figure 3.
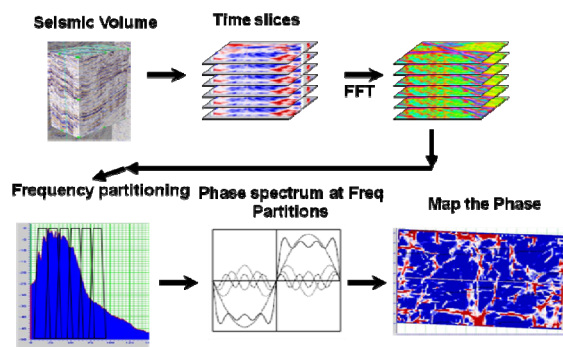

Figure 3. A schematic showing the implementation of the phase congruency algorithm to seismic data.

Karst Collapse Case Study

We analyzed a 3D dataset from the Boonsville area of north Texas. The wells and 3D seismic from this dataset are public domain, and available from the Bureau of Economic Geology at the University of Texas.

The geology of the area and exploration objectives of the Boonsville dataset have been fully described by Hardage et al. (1996).   In the Boonsville gas field, production is from the Bend conglomerate, a middle Pennsylvanian clastic deposited in a fluvio-deltaic environment. The Bend formation is underlain by Paleozoic carbonates, the deepest being the Ellenburger Group of Ordovician age. The Ellenburger contains numerous karst collapse features which extend up to 760 m from basement through the Bend conglomerate. These Karst collapse features have a significant effect on the producing events. It is therefore important to identify the karst collapse features from the seismic volume and we will do this using the phase congruency method. Figure 4 shows a set of composite slices (in the X, Y and Z directions) over the 3D seismic survey, where Figure 4(a) shows the original seismic survey and Figure 4(b) shows the phase congruency results.
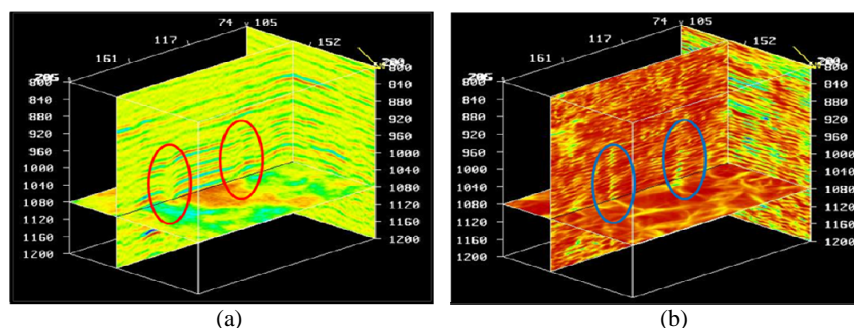

(a)   (b)

Figure 4. A vertical slice showing karst features superimposed on a horizontal slice at 1080 ms, roughly halfway through the karst collapse, where (a) shows the seismic volume and (b) shows the phase congruency volume.

On Figure 4(a), the Y-direction, or in-line, slice shows the karst features quite clearly (they are annotated with the red ellipses) but on the horizontal time slice they are not as clear. On Figure 4(b), the in-line slice shows the karst features even more clearly than on the seismic display (again, they are annotated with the red ellipses) and on the horizontal time slice they are also much clearer.

Conclusions

In this paper we implemented a new scheme for identifying discontinuities on seismic data slices, called phase congruency. As we discussed, the phase congruency approach has found application in the identification of features on images and is used in image processing for robot vision. However, the method had found little application in the seismic area and so we wanted to see if it could aid in the search for discontinuities on seismic time slices. We first described the theory of the phase congruency method. Next, we showed how the method works on a simple image consisting of an overlapping cylinder and cube. Finally, we applied the algorithm to a seismic example, and found that we could identify Karst collapse features very effectively.

References

Hardage, B.A., Carr, D.L., Lancaster, D.E., Simmons, J.L. Jr., Elphick, R.Y., Pendleton, V.M. and Johns, R.A., 1987, 3-D seismic evidence of the effects of carbonate karst collapse on overlying clastic stratigraphy and reservoir compartmentalization, GEOPHYSICS, 61, 1336-1350.

Kovesi, P.D., 2003, Phase congruency detects corners and edges: Proceedings of the Seventh Australasian Conference on Digital Image Computing Techniques and Applications (DICTA'03).